Title

Sensitivity of olive leaf turgor to air vapour pressure deficit correlates with diurnal maximum stomatal conductance

Authors

Rodriguez-Dominguez, CM
Hernandez-Santana, V
Buckley, TN
et al.

Publication Date

2019-07-01

DOI

10.1016/j.agrformet.2019.04.006

Peer reviewed

Agricultural and Forest Meteorology 272–273 (2019) 156–165

Contents lists available at ScienceDirect

Agricultural and Forest Meteorology

journal homepage: www.elsevier.com/locate/agrformet

Sensitivity of olive leaf turgor to air vapour pressure deficit correlates with diurnal maximum stomatal conductance

C.M. Rodriguez-Dominguez[a,*], V. Hernandez-Santana[a], T.N. Buckley[b], J.E. Fernández[a], A. Diaz-Espejo[a]

[a] Irrigation and Crop Ecophysiology Group, Instituto de Recursos Naturales y Agrobiología de Sevilla (IRNAS, CSIC), Avenida Reina Mercedes, 10, 41012, Sevilla, Spain
[b] Department of Plant Sciences, University of California, Davis, One Shields Ave, Davis, CA 95616, USA

ARTICLE INFO

Keywords:
Plant water stress indicator
Leaf turgor pressure
Stomatal conductance
Olive
Drought
Moderate water stress

ABSTRACT

Effective study and management of crops and forests would benefit greatly from useful plant-based indicators of the biological controls on evapotranspiration, and particularly stomatal conductance (g_s). Given the strong influence of g_s on bulk leaf water potential and turgor pressure (P), *in vivo* measurement of P may provide useful information about diurnal or seasonal dynamics of g_s. Moderate plant water stress affects the diurnal dynamics of P as leaf-to-air vapour pressure deficit (D) varies, and these dynamics correlate to g_s. Here, we explored relative changes in P in response to changes in D under mild drought conditions, and how these changes are linked to stomatal behaviour, and specifically to diurnal maximum g_s ($g_{s,max}$), one of the best indicators of plant water stress. We monitored ecophysiological and environmental variables, as well as a relative proxy for P, during three consecutive seasons in a hedgerow olive orchard where trees were supplied with different irrigation treatments to create well-watered and moderately water-stressed conditions. Our results demonstrated that the sensitivity of P to D correlated well with $g_{s,max}$ reached by the trees within a range in which variations in g_s are the main diffusional limitation to photosynthesis. We further showed that this correlation held under a wide range of meteorological conditions and soil water availability. This turgor proxy measurement, which is much easier to measure than g_s, can facilitate the use of $g_{s,max}$ as an indicator of plant water stress and evapotranspiration in agriculture and plant science research.

1. Introduction

Drought intensification worldwide due to climate change has increased the necessity of understanding how water stress affects the dynamics of plant-atmosphere vapor and carbon exchange through its effects on stomatal conductance (g_s). Current models are reasonably good at predicting diurnal dynamics of g_s relative to its diurnal maximum ($g_{s,max}$), using formulations with varying degrees of empiricism and mechanistic detail. However, most models rely on empirical parameterizations to capture how water stress drives shifts in $g_{s,max}$ at longer time scales of weeks, months and beyond (Buckley, 2017; Buckley and Mott, 2013; Damour et al., 2010). Thus, a reliable and accurate indicator for stress-related shifts in $g_{s,max}$ would be invaluable for quantifying impacts of water stress on transpiration, for applications ranging from precision irrigation of crops (Hernandez-Santana et al., 2016) to modelling crop photosynthesis and yield (Hernandez-Santana et al., 2018), to improving large-scale models of plant-atmosphere gas exchange (Rogers et al., 2017). Because $g_{s,max}$ integrates numerous internal (hydraulic conductance, osmotic adjustment, phytohormones) and external (atmospheric demand, soil water content) factors related to drought and avoids complexities related to diurnal dynamics of g_s, it is also a useful indicator of water stress in its own right (Correia et al., 1995; Flexas et al., 2004; Medrano et al., 2002).

Stomatal behaviour is closely related to the dynamics of leaf turgor (P) during the day: stomatal opening in the morning increases transpiration and reduces leaf water potential and, hence, turgor pressure (Ache et al., 2010). Dynamics of P, in turn, affect g_s via feedback regulation (Buckley, 2005; McAdam and Brodribb, 2016). Thus, plant-based measurement of leaf turgor may provide information useful for quantifying g_s and $g_{s,max}$. Plant-based sensors have been extensively used for precision irrigation scheduling of horticultural crops (Conejero et al., 2007; Cuevas et al., 2013; Fernández, 2017; Fernández et al., 2011, 2008, 2001; Intrigliolo and Castel, 2006; Ortuño et al., 2010), for validating the use of simplified forms of mechanistic models (Buckley et al., 2012) and for unravelling physiological processes (Bauer et al., 2013). One such sensor, the leaf patch clamp pressure probe ("ZIM

* Corresponding author. Current address: School of Biological Sciences, University of Tasmania, Private Bag 55, Hobart, 7001, Tasmania, Australia.
E-mail addresses: cmrdominguez@gmail.com, crdominguez@us.es (C.M. Rodriguez-Dominguez).

https://doi.org/10.1016/j.agrformet.2019.04.006
Received 2 November 2018; Received in revised form 16 March 2019; Accepted 7 April 2019

probe"), measures a relative proxy of bulk leaf turgor pressure (Ache et al., 2010; Ehrenberger et al., 2012b, 2012a; Rüger et al., 2010a). Due to the ZIM probe's simplicity and its applicability on nearly any plant species with flat leaves, it has been reliably used to monitor water status in several plant species and crops (Bader et al., 2014; Bramley et al., 2013; Fernández et al., 2011; Lee et al., 2012; Martínez-Gimeno et al., 2017; Rüger et al., 2010b; Westhoff et al., 2009) and to study the regulation of leaf water status (Ache et al., 2010; Bauer et al., 2013).

A common challenge with plant-based sensors is to relate their output to physiologically meaningful parameters in a consistent manner (Fernández, 2017, 2014a; Jones, 2007). A qualitative classification of diurnal curve shapes of ZIM probe outputs has proven useful as a plant water stress indicator under different plant water status and also under severe water stress (Marino et al., 2016; Martínez-Gimeno et al., 2017; Padilla-Díaz et al., 2018, 2016). Attempts to derive more meaningful water stress indicators for high plant water status and, hence, more related to stomatal function have been reported (Marino et al., 2016). However, a quantitative, physiologically based indicator of ZIM probe outputs has never been, to our knowledge, studied and demonstrated useful for studying regulation of plant water status under moderate stress.

Diurnal variations in turgor and g_s are driven by shifts in evaporative demand (leaf to air water vapor mole fraction difference, D), and, hence, the sensitivity of turgor to changes in D (dP/dD) should vary linearly with stomatal conductance (because $P \approx \psi_{soil} + \pi - g_s D/K$, where ψ_{soil} is soil water potential, π [≥ 0] is leaf osmotic pressure, and K is plant hydraulic conductance). More specifically, if dP/dD is expressed instead as dP_{rel}/dD, where P_{rel} is P normalized relative to its seasonal range, the resulting quantity should be approximately proportional to diurnal $g_{s,max}$ and inversely proportional to the seasonal maximum of transpiration rate (E_{max}), i.e.,

$$\frac{dP_{rel}}{dD} \propto -\frac{g_{s,max}}{E_{max}} \quad (1)$$

Eq. (1), which is derived in the Appendix as Eq. (A8), suggests that variations in leaf turgor with respect to D could serve as a sensor for changes in $g_{s,max}$ under water stress.

The objective of this study was to test the hypothesis that the sensitivity of ZIM probe output (Z) to D (i.e., dZ/dD) can be used as a proxy for dP_{rel}/dD in order to detect variations in $g_{s,max}$ and plant water stress during moderate soil water deficit in olive, a woody crop species. We quantified dZ/dD and compared it with two estimates of variation in $g_{s,max}$ during water stress: (i) fortnightly measurements of $g_{s,max}$ in well-watered and moderately water-stressed olive trees growing in a hedgerow orchard during three consecutive irrigation seasons, and (ii) daily $g_{s,max}$ estimated from sap flux density data (Hernandez-Santana et al., 2016) recorded during an entire season.

2. Material and methods

2.1. Experimental design and water stress conditions

The present study was performed from 2010 to 2012 in a commercial hedgerow olive orchard (*Olea europaea* L., *cv.* Arbequina) near Seville, Spain (37° 15′ N, −5° 48′ W). The orchard was planted with 1667 trees ha^{-1} in 2007. The diverse objectives of the research projects based on this orchard allowed us to combine a range of data to test our hypothesis. From 2010–2012, different regulated deficit irrigation strategies and their effects on water productivity, fruit yield and oil production were tested (Fernández et al., 2018, 2013; Padilla-Díaz et al., 2016). Concomitantly, experiments exploring the use of plant water stress indicators for irrigation scheduling (Cuevas et al., 2013; Fernández, 2014a; Fernández et al., 2011; Hernandez-Santana et al., 2016; Padilla-Díaz et al., 2016; Rodriguez-Dominguez et al., 2012) and the application of mechanistic models to manage water use (Diaz-Espejo et al., 2012) were also conducted. The orchard characteristics, irrigation strategies and experimental design were explained in detail by these authors. Specifically for the present work, two regulated deficit irrigation (RDI) treatments were imposed in the orchard: 60RDI, scaled to a total irrigation amount of 60% of the irrigation needs (IN); and 30RDI, scaled to a total of 30% of IN, where IN = $ET_c - P_e$, ET_c being the maximum potential crop evapotranspiration calculated with the crop coefficient approach (Allen et al., 1998) and P_e the effective precipitation calculated as 75% of the precipitation recorded in the orchard (Orgaz & Fereres, 2001). Control treatments for all the years aimed to replace 100% of IN. A randomized block design was used with four 12 m × 16 m plots per treatment, with the exception of the Control treatment in 2010, for which only one plot was available. This design was based on previous measurements of the soil properties at the experimental site (Diaz-Espejo et al., 2012). Each plot contained eight central trees, where the measurements were made, surrounded by 24 border trees. For the present study, we only analysed the plots where plant-based sensors were installed; i.e., three out of the four plots per treatment. The irrigation seasons spanned from May to October.

The Control and RDI treatments generated well-watered and moderately water-stressed conditions, respectively, that allowed us to test our hypothesis within the water potential range of stomatal function of the plants. Threshold values for these olive trees of stem water potentials below *ca.* -1.7 MPa (Fernández et al., 2011) and maximum stomatal conductance below 0.1 mol m^{-2} s^{-1}, when biochemical limitations to photosynthesis start to occur (Flexas and Medrano, 2002), are considered severe water stress conditions. ZIM probe output has been classified qualitatively into three categories (‘State I’, ‘State II’ and ‘State III’, see Fig. S3 for an example of each State), based on the shape of the diurnal curve of probe output. These ‘States’ have been related to ranges of stem water potential. Thus, in olive, shapes of diurnal curve of probe outputs likely identified as ‘State I’ were observed when stem water potential (ψ_{stem}) > -1.2 MPa, ‘State II’ when -1.2 MPa > ψ_{stem} > -1.7 MPa, and ‘State III’ when ψ_{stem} < -1.7 MPa (Fernández et al., 2011; Padilla-Díaz et al., 2016). However, our long experience working with ZIM probes (Dreux et al., 2017; Ehrenberger et al., 2012b; Fernández, 2017, 2014a, Fernández et al., 2018, 2011, Padilla-Díaz et al., 2018, 2016; Rodriguez-Dominguez et al., 2012), showed us that some exceptions occur and some trees with slightly lower values than those threshold values still behave qualitatively as moderately water-stressed, and even well-watered, trees, based on leaf turgor measured with ZIM probes (i.e. ‘State I’). The physiological basis behind these transitions between ‘States’ remains still unclear. Notwithstanding, what we already know is that in ‘State II’ and ‘State III’ the relationship between the probe output and leaf turgor pressure start to be or is completely lost, so any relationship with leaf water status appears to be inconsistent (Ehrenberger et al., 2012b), which may explain differences on the range of ψ_{stem} that lead to transitions between ‘States’ found in olive under different conditions (Marino et al., 2016). For this study, we decided to use only data from plants under moderate water stress, defined as stem water potentials above the turgor loss point (‘State I’) (Ehrenberger et al., 2012b) and within the range of stomatal function of the plants. The minimum values of stem water potential and maximum stomatal conductance from these plants were -2.11 ± 0.06 MPa and 0.07 ± 0.01 mol m^{-2} s^{-1}, respectively (means ± SE across three growing seasons).

Weather variables for all the experimental years were monitored by a Campbell weather station (GRWS100 System, Campbell Scientific Ltd., Shepshed, UK) installed in the centre of the experimental area. The meteorological sensors were installed at 3 m above the trees and average values of air temperature (T_a), photosynthetic photon flux density (PPFD) and relative humidity (RH) were recorded every 30 min. T_a and RH were used to estimate leaf to air water vapor mole fraction difference (D) (Buck, 1981).

Table 1
Conditions during maximum stomatal conductance ($g_{s,max}$) measurements performed fortnightly at the hedgerow olive orchard for the three consecutive irrigation season (2010, 2011 and 2012). Average values ± standard deviations are presented for each year.

Variables	Years	Values
CO_2 concentration (μmol mol^{-1})	2010	381.3 ± 4.2
	2011	386.4 ± 9.4
	2012	392.9 ± 6.4
Chamber radiation (μmol m^{-2} s^{-1})	2010	1288.4 ± 289.8
	2011	1204.3 ± 292.1
	2012	1102.6 ± 370.6
Leaf temperature (°C)	2010	32.2 ± 2.9
	2011	31.5 ± 3.3
	2012	31.6 ± 3.8

2.2. Plant measurements

Once every two weeks during each irrigation season, plant water status and gas exchange were monitored. The midday stem water potential (ψ_{stem}) was measured with a Scholander-type pressure chamber (PMS Instrument Company, Albany, Oregon, USA) on healthy, fully developed leaves from the inner part of the canopy wrapped in aluminium foil for ca. 2 h before the measurements. Maximum stomatal conductance to H_2O ($g_{s,max}$) was measured fortnightly in all plots and treatments during each season between 0800 and 0930 Greenwich Mean Time (GMT), i.e. two hours less than the local time, using an open flow gas exchange system with a 2 cm × 3 cm chamber (IRGA Li-6400, LI-COR, Lincoln, NE, USA). Olive leaves did not fill the whole chamber, so the exact leaf area was drawn on acetates and measured later to correct the final measurement. Preliminary measurements demonstrated that stomatal conductance (g_s) measured at these times of the day (during the morning and before midday) represented $g_{s,max}$ reliably (Diaz-Espejo et al., 2018; Fernández et al., 1997; Rodriguez-Dominguez et al., 2016). Chamber radiation, temperature and CO_2 concentration matched ambient conditions (Table 1). For both plant water status and gas exchange monitoring, we measured one leaf per tree in two trees per plot, near the instrumented tree, and averaged results within each plot (three plots per treatment).

Three diurnal measurement cycles were also conducted (one in 2011 and two in 2012), comprising instantaneous measurements of stomatal conductance to H_2O (g_s) at 1.5–3 h intervals from dawn to sunset using the same gas exchange system as for $g_{s,max}$ measurements. Chamber radiation, temperature and CO_2 concentration matched ambient conditions. Measurements were completed within 1–2 min of enclosing the leaf in the chamber, to ensure measured g_s was indicative of the value prevailing prior to measurements. Three leaves in two plots of the Control treatment for each point were measured on July 20th 2011, and four leaves in one Control plot were measured on June 25th and August 3rd 2012.

In 2012, plant hydraulic conductance (K) was calculated from fortnightly measurements of $g_{s,max}$ and soil-to-leaf water potential gradient as:

$$K = \frac{g_{s,max} D}{\psi_{soil} - \psi_{leaf}}, \quad (2)$$

where ψ_{soil} is the soil water potential and ψ_{leaf} is the leaf water potential measured at midday. The use of ψ_{leaf} at midday was previously tested in our trees and conditions and did not present significant differences from ψ_{leaf} at the time of $g_{s,max}$, agreeing with abundant literature in olive showing the same trend (Diaz-Espejo et al., 2018; Fernández et al., 1997; Rodriguez-Dominguez et al., 2016; Torres-Ruiz et al., 2013). Leaf water potential at predawn was used as an estimate of ψ_{soil}. Leaves for both water potentials were sampled from representative current-year branches and measured with a Scholander-type pressure chamber.

In addition, pre-dawn leaf osmotic pressure (π) was measured on the same dates and using the same number of replicates (n = 3) as plant water status and gas exchange measurements in 2012. Mature, fully expanded leaves were cleaned, packed in aluminium foil and immediately frozen in liquid nitrogen. One 7-mm diameter disc per leaf was sampled between the midrib and margin with a cork borer, punctured 15–20 times with forceps to speed equilibration and immediately loaded in a C-52 thermocouple psychrometer chamber (Wescor Inc., Logan, UT, USA) connected to a datalogger (PSYPRO, Wescor). Equilibrium time in the chambers was *ca.* 30 min. π measurements were corrected by using the regression model proposed by Bartlett et al. (2012) to account for apoplastic dilution and wall solute enrichment.

2.3. ZIM probes

Relative changes in leaf turgor pressure were recorded *in situ* with the non-invasive, online-monitoring leaf patch clamp pressure probe ("ZIM probe", but also found in the literature as LPCP probe, YARA-ZIM probe or, recently, as YARA-Water sensor, YARA-ZIM Plant Technology GmbH, Hennigsdorf, Germany). The principle of the magnetic ZIM probe was described in detail by Westhoff et al. (2009) and Zimmermann et al. (2008). Briefly, a small patch of an intact leaf is used as a sensing element for measuring relative changes of turgor pressure in the entire leaf tissue. The leaf patch must be in hydraulic and osmotic equilibrium with its surrounding. The leaf is clamped between two metal pads in which two magnets are integrated. The lower pad contains a silicone-embedded temperature-independent pressure sensor chip. The magnetic pressure exerted on the leaf patch can be altered by changing the distance between the two magnets. Relative leaf turgor pressure is determined by measuring the pressure transfer function of the leaf patch, i.e., by measuring the leaf patch pressure output, P_p, upon application of a constantly kept external magnetic pressure (P_{clamp}). The attenuation of the applied external pressure and thus P_p depends on the magnitude of the turgor pressure of the leaf (P) which is opposed to P_{clamp}. That implies that P_p is low at high P and high at low P. Detailed analyses (Ehrenberger et al., 2012b; Westhoff et al., 2009; Zimmermann et al., 2008) showed that P_p is a power function of P, with a negative exponent. The signals are sent wirelessly by transmitters (connected by cable with the probe) to a controller which transfers the data to a GPRS modem linked to an Internet server. P_p was recorded every 5 min.

At the beginning of each irrigation season, three ZIM probes per treatment (one ZIM probe per tree and plot in three plots, n = 3) were installed. In the Control plot of 2010, one representative tree was instrumented. Details on the clamping procedure are given by Fernández et al. (2011). The probes were clamped on the eastern leaves of the canopy at about 1.5 m above ground. Since initial P_{clamp}, and thus initial P_p, in the turgescent state (early in the morning) can vary between leaves (10–25 kPa approx.), P_p, previously smoothed by using the 9-point FFT Filter routine in OriginPro 8.1 (OriginLab, Northampton, MA, USA), was normalized as shown in Eq. (3) below, to enable outputs to be averaged and compared between probes. Averages of the probe outputs were necessary in this study since the trees were not individually monitored, i.e. ecophysiological variables were not measured on the same trees with ZIM probes installed but on the same plot and treatment. Thus, normalization of P_p was compulsory to compare and average ZIM probe outputs. However, for further applications, trees can be individually monitored so the actual value of P_p can be used without the need of comparing with other probes and, in that case, no normalization would be needed. The normalized P_p calculation was:

$$Z = \frac{P_p - P_{p,min}}{P_{p,max} - P_{p,min}} \quad (3)$$

where P_p is the actual value of the probe output. $P_{p,min}$ and $P_{p,max}$ are the seasonal minimum and maximum values (i.e. maximum and

minimum leaf turgor pressure, respectively) from periods of each season in which the diurnal patterns of ZIM probe outputs corresponded to well hydrated leaves or turgescent leaves, i.e., curves in which P_p increased during the morning (P decreased), reached the maximum peak at around midday and decreased (P increased) during the afternoon until the minimum peak at night, or 'State I'. Unrealistic P_p peak values due to bad weather conditions and diurnal P_p curve shapes identified as 'State II' and 'State III' (see Section 2.1) were not considered. Thus, Z values captured the variation in P_p values but ranged between 0 and 1, meaning proportions of change in P_p.

2.4. Deriving the leaf turgor pressure-based indicator

The physiological plant-based indicator examined in this study is not P_p itself, but the sensitivity of its normalized value (Z) to D; i.e., dZ/dD. Supporting Information File Figure S4 contains a graphical representation of the calculation of dZ/dD. We excluded data for which PPFD was below 150 μmol m^{-2} s^{-1} to exclude nocturnal stomatal opening. As indicated by Eq. (1), dZ/dD is predicted to be proportional to $g_{s,max}$. dZ/dD may also vary as g_s fluctuates below $g_{s,max}$; preliminary work found that Z *vs.* D approximated a bi-linear relationship during the morning of each day, with one slope during early to mid-morning and a shift to a more shallow slope from mid-morning to midday or early afternoon, after which dZ/dD approximated or became negative (Fig. S4d). After $g_{s,max}$ is reached in olive trees, which occurs during the morning (Diaz-Espejo et al., 2018; Fernández et al., 1997), g_s starts to oscillate (López-Bernal et al., 2018). Thus, to focus only on the moment of the day when $g_{s,max}$ occurs and to avoid an influence of stomatal closure or oscillations on the dynamics of P_p, and hence of Z, which occur from the afternoon through the rest of the day (Fernández et al., 2011), we focused on a period from early morning (just after stomatal opening) to early afternoon, excluding the period of the day when dZ/dD became negative. We thus characterized dZ/dD by piecewise linear regression of Z *vs.* D for each day using the R (R Core Team, 2017) package 'segmented' (Muggeo, 2008, 2003), which gave the D values at which dZ/dD changed and the two values of dZ/dD for each experimental day and ZIM probe: one high (morning) value and one lower (mid-morning or early afternoon) value. dZ/dD values were then averaged per treatment (i.e., $n = 3$).

2.5. Sap flux density measurements

To test our hypothesis in a wider range of plant water status, we derived a surrogate of g_s from sap flux density data of 2012. Sap flux density (J_s, mm h^{-1}) values were obtained using the Compensation Heat Pulse (CHP) method (Green et al., 2003). Details on the calibration and testing of the technique for the olive tree, as well as on data analysis, are given in Fernández et al. (2006, 2001). The same trees instrumented with ZIM probes, i.e., one tree per plot in three plots per treatment (Control, 60RDI and 30RDI), were instrumented at the beginning of the season with two sap flow probe sets, at the east and west facing sides of the trunk and at 0.3–0.4 m aboveground. Each probe set measured J_s at 5, 10, 15 and 20 mm depths below the cambium, every half hour for the entire experimental period. A CR10X datalogger connected to an AM25 T multiplexer (Campbell, Campbell Scientific Ltd., Shepshed, UK) was used to release the heat pulses and collect the probe outputs. Hernandez-Santana et al. (2016) reported a good agreement between J_s (measured at 5 mm below the cambium) divided by D and $g_{s,max}$, both from the same time of day (between 8:00 and 9:30 GMT), measured fortnightly during the irrigation season. Thus, we used those data (J_s at 5 mm below the cambium divided by D) to extend the $g_{s,max}$ derived from sap flux density ($g_{s,maxSF}$) data to the entire season.

2.6. Statistics

To test whether the slope of dZ/dD *vs.* $g_{s,max}$ was significantly different between seasons, we used the lm() function of R (R Core Team, 2017), treating dZ/dD as the response variable and the interaction $g_{s,max}$ and season as the independent variable. In addition, one-way repeated measures analysis of variance (ANOVA) was used to determine the statistical significance among π values in 2012 across treatments and dates, i.e. the effect of treatments and different days on π. Mean comparisons were performed by *post-hoc* Tukey's test ($P < 0.05$).

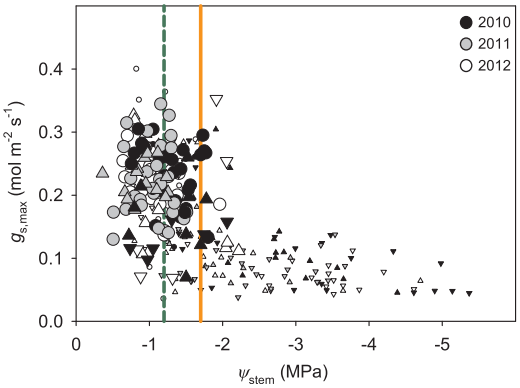

Fig. 1. Relationship between maximum stomatal conductance ($g_{s,max}$) and midday stem water potential (ψ_{stem}) measured in 2010, 2011 and 2012 at the olive hedgerow orchard. Black symbols correspond to 2010, grey symbols to 2011, white symbols to 2012, and different symbol types indicate different irrigation treatments (circles = Control, triangles up = 60RDI, triangles down = 30RDI). Each point represents a plot where these variables were measured in two trees and one leaf per tree close to the instrumented tree. The green dashed and orange solid reference lines correspond to ψ_{stem} = -1.2 MPa and ψ_{stem} = -1.7 MPa, respectively. These threshold values likely produce transitions to 'State II' (-1.2 MPa > ψ_{stem} > -1.7 MPa) and 'State III' (ψ_{stem} > -1.7 MPa) considering a qualitative classification of the diurnal curves of the ZIM probe outputs according to Fernández et al. (2011) and Padilla-Díaz et al. (2016). Smaller symbol sizes represent the dataset excluded from our analyses, and bigger symbol sizes represent the dataset used to test our hypothesis covering a range of ψ_{stem} down to -2.11 MPa and $g_{s,max}$ down to 0.07 mol m^{-2} s^{-1}. (For interpretation of the references to colour in this figure legend, the reader is referred to the web version of this article).

3. Results

Stomatal control at the hedgerow olive orchard during the three consecutive seasons in differently irrigated trees resulted in a highly scattered relationship between maximum stomatal conductance ($g_{s,max}$) and midday stem water potential (ψ_{stem}) for ψ_{stem} > -1.7 MPa (Fig. 1). Within this range of ψ_{stem}, $g_{s,max}$ varied from *ca.* 0.3 to 0.1 mol m^{-2} s^{-1}, which represented a 50% decrease in net assimilation rate of CO_2 (A_N) (Supporting Information File Figure S5). Within this range, diurnal patterns of ZIM probe outputs (P_p, or Z as its normalized value) showed that leaves remained well above the turgor loss point (Fig. S4).

Diurnal stomatal conductance increased in the morning until $g_{s,max}$ was reached, which coincided with a distinct change in the slope of Z *vs.* D (Fig. 2). The two slopes – a greater slope prior to this point, and a smaller slope after this point – were used as dZ/dD for further analysis. The morning value of dZ/dD was more seasonally variable than the mid-morning to early afternoon value (Supporting Information File Figure S6) and was strongly correlated with $g_{s,max}$ (Fig. 3; $P < 0.05$ in all cases), whereas the mid-morning to early afternoon value of dZ/dD was uncorrelated with $g_{s,max}$ (Supporting Information File Figure S7). Therefore, for subsequent analyses, we focused exclusively on the morning values of dZ/dD. The relationships across seasons that determined these morning values of dZ/dD, i.e. slopes of Z *vs.* D, were all highly significant (with $r^2 > 0.80$ and $P < 0.05$ in all cases). Consistent with Eqn 1, the intercept of dZ/dD *vs.* $g_{s,max}$ was not significantly different from zero for all experimental years (0.004 ± 0.006 kPa^{-1};

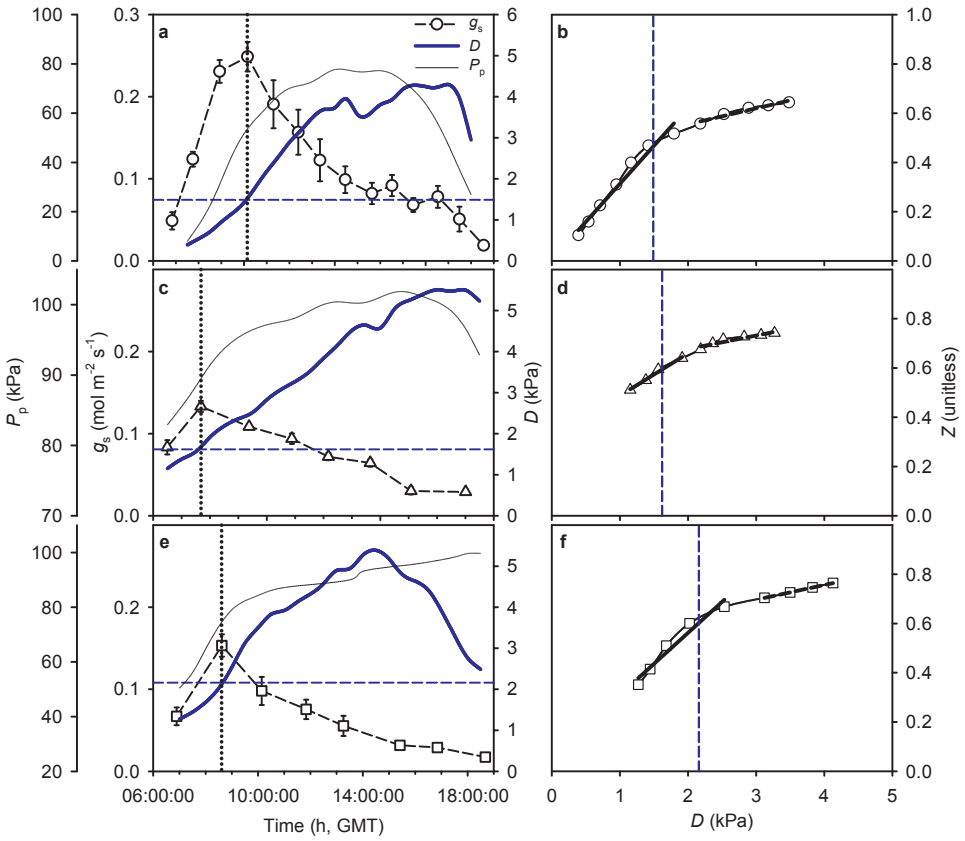

Fig. 2. Three diurnal measurement cycles performed at the olive hedgerow orchard showing the agreement between the time of maximum stomatal conductance ($g_{s,max}$) occurrence and the vapour pressure deficit (D) value at which the slope of normalized ZIM probe output (Z) *vs.* D relationships changed. Panels at left show the diurnal (from sunrise to sunset) leaf patch pressure (P_p) outputs (black thin solid lines), stomatal conductance to H_2O (g_s) values (symbols and dashed lines) and D values (blue thick solid lines) measured on July 20th 2011 (a), June 25th 2012 (c) and August 3rd 2012 (e). In 2011, each g_s point corresponded to three leaves measured in two plots of the Control treatment, and in 2012, each g_s point corresponded to four leaves measured in one Control plot. The vertical dotted lines represent the time in which $g_{s,max}$ was measured and the horizontal blue dashed lines show the D values when those $g_{s,max}$ occurred. Panels at right represent the Z *vs.* D relationships from July 20th 2011 (b), June 25th 2012 (d) and August 3rd 2012 (f) and using the values of Z recorded at the same Control treatment. The vertical blue dashed lines correspond to the breakpoints (D values) derived from the piecewise regression analyses performed (R package 'segmented', see Materials and Methods for details), which coincided with the slope changes of the Z *vs.* D relationships. When those D values were plotted as horizontal blue dashed lines on the panels at left, they agreed with the moment at which $g_{s,max}$ occurred (horizontal blue dashed lines exactly crossed vertical dotted lines). Solid bold lines at right panels indicate the linear regressions used to derive the slopes from the Z *vs.* D relationships (dZ/dD) and the dashed bold lines show the second linear regressions that were not used. Breakpoints or D values derived from the piecewise regression analyses: July 20th 2011 = 1.49 kPa (a, b); June 25th 2012 = 1.62 kPa (c, d); August 3rd 2012 = 2.16 kPa (e, f). (For interpretation of the references to colour in this figure legend, the reader is referred to the web version of this article).

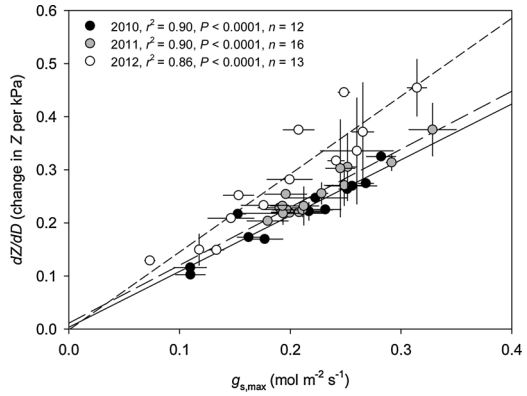

Fig. 3. Relationships between variations in normalized ZIM probe outputs per vapour pressure deficit changes during the morning (dZ/dD) and maximum stomatal conductance ($g_{s,max}$) measured by gas exchange at the hedgerow olive orchard during three experimental seasons. Each point represents the average of three plots monitored along each year with error bars as SE. Slope values: 1.05 (2010), 1.09 (2011) and 1.47 (2012). Intercept values: 0.003 (2010), 0.011 (2011) and -0.001 (2012).

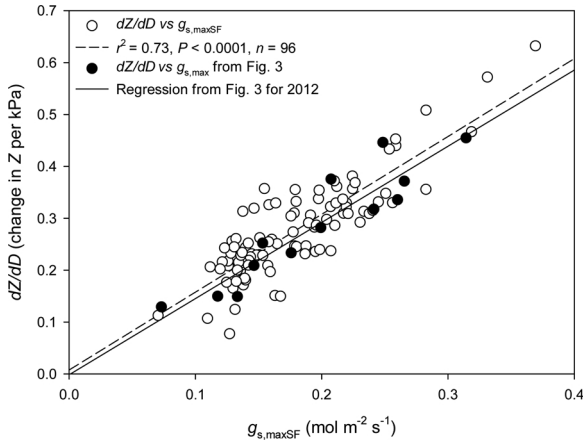

Fig. 4. Relationship between variations in normalized ZIM probe outputs per vapour pressure deficit changes (dZ/dD) and maximum stomatal conductance derived from sap flux density data ($g_{s,maxSF}$ = J_s at 5 mm below the cambium divided by D) measured in olive trees at the hedgerow orchard in 2012. Each point represents the average of three trees per treatment in the three treatments monitored along the experimental season from May to October. The $g_{s,maxSF}$ values used here were those at the same time of the day dZ/dD were considered, i.e. the time when the slopes from Z *vs.* D relationships changed. Fitted linear equation: dZ/dD = 1.50 $g_{s,maxSF}$ + 0.008.

P > 0.05; Fig. 3). The slope of dZ/dD *vs.* $g_{s,max}$ was slightly, but not significantly, greater in 2012 (1.47) than in 2010 and 2011 (1.05 and 1.09, respectively; Fig. 3).

We used a sap flux-based surrogate of $g_{s,max}$ ($g_{s,maxSF}$) to assess the relationship between dZ/dD and $g_{s,maxSF}$ for an entire experimental season (2012), comprising a wider range of environmental and water soil conditions than possible with our gas exchange data. The resulting relationship, using morning values of dZ/dD, was linear and strongly significant (Fig. 4, r^2 = 0.73, P < 0.0001, n = 96), with an intercept not significantly different from zero, consistent with Eq. (1). Furthermore, the slope of dZ/dD *vs.* $g_{s,maxSF}$ was similar to that found using gas

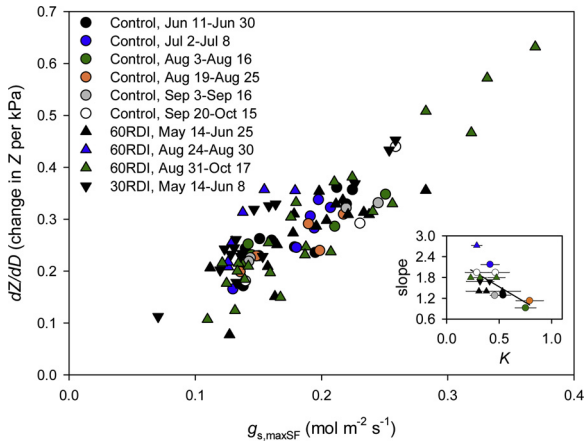

Fig. 5. Relationship between dZ/dD and $g_{s,maxSF}$ presented in Fig. 4 showing each treatment (Control = circles, 60 RDI = triangles up, 30 RDI = triangles down) and periods (different colours) within the experimental season separately. The inset graph represents the relationship between the slope values derived from each separate group and the plant hydraulic conductance (K, mmol $s^{-1}\,m^{-2}\,MPa^{-1}$) calculated using the plant measurements performed within the same periods for which the slopes were derived in 2012 ($r^2 = 0.43$, $P = 0.004$) (see Material and Methods for details). Each point, with the same colour and symbol type than the period, refers to a measurement day in which K was measured in three plots per treatment ($n = 3$) ± SE (For interpretation of the references to colour in this figure legend, the reader is referred to the web version of this article.).

exchange-based $g_{s,max}$ (1.50 and 1.47, respectively).

To gain insight into the reason for the slight differences in the slope of dZ/dD *vs.* $g_{s,max}$ between years (Fig. 3), we examined how that slope varied among months and irrigation treatments in the more intensive dataset based on sap flux-derived $g_{s,max}$ (Fig. 5). As predicted by Eqns A10 and A11, we found that the slope of dZ/dD *vs.* $g_{s,maxSF}$ was significantly and negatively correlated with K (calculated using Eq. (2) considering fortnightly K values) (inset graph in Fig. 5). Although we did not measure seasonal variations in diurnal minimum leaf water potential ($\psi_{leaf,min}$), we found that a proxy for $\psi_{leaf,min}$ – leaf osmotic pressure (π) – did not differ among months or treatments (Table 2).

Table 2
Osmotic pressures measured at the olive hedgerow orchard (π) during 2012 for the same periods presented in Fig. 5 (same symbols and colors are shown to easily identify each period). Means ± SE are presented. Number of replicates were three in all cases except for Control 23-Aug-2012 when only two plots were measured. No significant differences were found (one-way repeated measures ANOVA, $P > 0.05$).

Treatments	Measurement day	π MPa
Control ●	*28-Jun-2012*	1.68 ± 0.14
●	*12-Jul-2012*	2.05 ± 0.27
●	*9-Aug-2012*	2.06 ± 0.05
●	*23-Aug-2012*	2.11 ± 0.30
●	*6-Sep-2012*	1.90 ± 0.15
○	*4-Oct-2012*	1.65 ± 0.03
○	*18-Oct-2012*	1.79 ± 0.16
60 RDI ▲	*31-May-2012*	2.00 ± 0.28
▲	*14-Jun-2012*	1.86 ± 0.21
▲	*28-Jun-2012*	1.63 ± 0.24
▲	*23-Aug-2012*	2.16 ± 0.11
▲	*6-Sep-2012*	2.16 ± 0.20
▲	*4-Oct-2012*	1.65 ± 0.03
▲	*18-Oct-2012*	1.84 ± 010
30 RDI ▼	*9-May-2012*	1.96 ± 005
▼	*31-May-2012*	1.79 ± 019

4. Discussion

Stomata have the decisive role in controlling water loss and carbon gain at plant and global scales (Hetherington and Woodward, 2003). Thus, the ability to monitor stomatal conductance *in vivo* would be invaluable for understanding, monitoring and managing plant water stress. We hypothesized, based on a novel relationship that we derived from water relations theory, that the normalized sensitivity of leaf turgor to vapour pressure deficit (D) should be proportional to the diurnal maximum of stomatal conductance ($g_{s,max}$) as $g_{s,max}$ varies seasonally in relation to cycles of moderate water stress. Our data strongly supported this hypothesis: changes in dZ/dD – where Z is a surrogate for normalized leaf turgor, measured with a simple plant-based sensor – correlated strongly with $g_{s,max}$ in olive trees under both well-watered conditions and moderate soil water deficits, and across three consecutive seasons. We found similar results using an extended database in which a continuous record of $g_{s,max}$ was estimated from sap flux density data along one growing season. We also identified the key physiological variables that should drive variations in the slope of dZ/dD *vs.* $g_{s,max}$ (namely, the seasonal maximum transpiration rate, which depends on plant hydraulic conductance and minimum leaf water potential). Our results thus demonstrate the feasibility of monitoring $g_{s,max}$ *in vivo* using a sensor that measures a surrogate of leaf turgor pressure and has a rigorous physiological basis (Fernández, 2017, 2014a; Jones, 2007).

4.1. The physiological basis of the conservative relationship between dZ/dD and $g_{s,max}$

For plant-based sensors to have broad utility, it must be possible to link their output to physiological processes or traits in a consistent way. The strong relationship revealed in this study between the value of dZ/dD in the morning and the value of $g_{s,max}$ satisfies this requirement, because it was predicted from physiological principles (see derivation of Eq. 1 in the Appendix). The relationship arises because the sensitivity of leaf turgor to D is mostly driven by the absolute values of stomatal conductance and hydraulic conductance (McAdam and Brodribb, 2015, 2014; Rodriguez-Dominguez et al., 2016). Two more subtle issues require attention, however. First, it is not obvious why dP/dD (and dZ/dD) should be fairly constant as D and g_s covary during the morning of a single day, before g_s reaches $g_{s,max}$. To interpret this, consider the following equation (Eq. (A7)):

$$\frac{dP_{rel}}{dD} = -\frac{g_s}{E_{max}}\left(1 + \frac{d\ln g_s}{d\ln D}\right) \quad (4)$$

where P_{rel} is leaf turgor normalized by its seasonal range (normalized ZIM probe output, Z, is an estimate of 1 - P_{rel} [Eqn A9]). When $g_s = g_{s,max}$, $d\ln g_s/d\ln D = 0$, because the rate of change of g_s with respect to any parameter is zero when g_s is at its maximum. The fact that dZ/dD is fairly conservative when g_s is approaching $g_{s,max}$ during the morning suggests that the product $g_s{\cdot}(1 + d\ln g_s/d\ln D)$ is likewise somewhat conservative. This is intuitively reasonable, because by definition g_s is approaching its maximum during that period, so that its relative rate of change ($d\ln g_s/d\ln D$) should be decreasing. As soon as $g_{s,max}$ is achieved, the leaf turgor pressure becomes low enough to produce stomatal closure, leading to a decrease in dZ/dD.

The second issue involves the fact that the slope of dZ/dD *vs.* $g_{s,max}$ was relatively conservative across irrigation treatments and even between years. Eqs. (1) and (4) predict the slope should be inversely related to the seasonal maximum transpiration rate, E_{max}, which is equal to $K(\psi_{soil} - \psi_{leaf,min})$, where K is whole-plant leaf-specific hydraulic conductance and $\psi_{leaf,min}$ is the seasonal minimum leaf water potential. This suggests that the slope of dZ/dD *vs.* $g_{s,max}$ should be conservative in species that tend to maintain constant $\psi_{leaf,min}$ over the growing season, and which have low hydraulic vulnerability to cavitation (i.e., K that

does not vary in relation to typical diurnal variation in water potential). Olive meets both of these requirements (Cuevas et al., 2010; Rodriguez-Dominguez et al., 2018; Torres-Ruiz et al., 2013), so it is unsurprising that the slope of *dZ/dD vs.* $g_{s,max}$ is so conservative in this species. However, even in species that exhibit pronounced variation in $\psi_{leaf,min}$ in relation to soil moisture, any decline in *K* at low water potential would tend to counteract the effect of more negative $\psi_{leaf,min}$, minimizing shifts in E_{max} and thereby preserving a conservative slope between *dZ/dD* and $g_{s,max}$. Whether this in fact holds for species that exhibit pronounced seasonal variation in *K* and/or $\psi_{leaf,min}$ is unknown, and the matter deserves further attention.

The slope of *dZ/dD vs.* $g_{s,max}$ did change slightly between seasons, being higher in 2012 than in 2010 and 2011. This is consistent with the fact that seasonal E_{max} was lower in 2012 than in 2011 (1.52 *vs.* 1.73 mmol m^{-2} s^{-1}, respectively, averaged across treatments and periods of study), which may, in turn, reflect shifts in *K*. Indeed, *K* estimated from sap flow measurements and soil-to-leaf water potential gradients according to Diaz-Espejo et al. (2012) was much smaller in 2012 than in 2011 (0.9 *vs.* 1.7 mmol m^{-2} s^{-1} MPa^{-1}, respectively), partly due to an increase in leaf area in 2012 taking into account only the Control treatment (12 m^2 *vs.* 9 m^2 in 2011) (Fernández et al., 2013). In our study, the slope of *dZ/dD vs.* $g_{s,max}$ estimated from sap flux and *D* ($g_{s,maxSF}$) correlated well with changes in *K* across periods and treatments during 2012. Although E_{max} also depends on ψ_{soil} - $\psi_{leaf,min}$, neither ψ_{soil} nor leaf osmotic pressure (a proxy for $\psi_{leaf,min}$ in olive, which approaches the turgor loss point during the season (Diaz-Espejo et al., 2018)) varied significantly in the periods and trees considered in this study, suggesting that *K* was mostly responsible for the observed variation in E_{max} and thus for the variation in the slope of *dZ/dD vs.* $g_{s,max}$.

4.2. Comparison of methods for monitoring stomatal conductance in situ

Because stomatal conductance integrates both external (atmospheric demand, soil water content) and internal (ABA, osmotic adjustment, hydraulic conductance) factors related to drought, and because stomatal closure is one of the earliest responses to drought (Martin-StPaul et al., 2017) and the primary limitation to photosynthesis (Flexas and Medrano, 2002), it is a critical parameter in the study of water stress responses. However, measuring g_s *in situ* by gas exchange is highly time consuming and impractical for applications requiring extended monitoring of g_s, such as irrigation scheduling or estimating ET. The method proposed here, in which diurnal maximum g_s is estimated from a leaf turgor-related sensor, has strengths and advantages over the estimation of g_s from sap flow and micrometeorological data. Both methods appear capable of faithfully estimating g_s (in the case of sap flow) or $g_{s,max}$ (in the case of the ZIM probe method described here): indeed, it is noteworthy that the slopes of *dZ/dD vs.* $g_{s,max}$ estimated by gas exchange and sap flow were so similar, which indicates a good match between g_s estimated from sap flux density and gas exchange, further confirming the robustness of sap flux-based g_s estimation (Hernandez-Santana et al., 2016). Sap flow-based g_s has the obvious advantage over ZIM probes of providing a near-continuous measure of g_s. This can be used to estimate photosynthesis (Hernandez-Santana et al., 2018) and to address questions involving diurnal responses, such as mechanisms of stomatal regulation, and it reduces uncertainties in using the Penman-Monteith equation to estimate evapotranspiration (Hernandez-Santana et al., 2018, 2016). However, estimating g_s from sap flow requires the monitored trees to be highly coupled to the atmosphere (Jarvis and Mcnaughton, 1986), and further requires accurate estimation of sapwood area as well as integration of sap flow velocity across the sapwood profile. By contrast, ZIM probes do not have these requirements, and their simplicity allows them to be applied to nearly any species with flat leaves, ranging from woody to herbaceous species. Furthermore, if the objective of quantifying g_s is to evaluate water stress, diurnal patterns are more difficult to interpret, and $g_{s,max}$ is an adequate indicator of water stress, and perhaps even a superior one (Correia et al., 1995; Flexas et al., 2004; Medrano et al., 2002). The utility of $g_{s,max}$ as a water stress indicator may reflect the fact that, when g_s is at its diurnal maximum, both turgor- and non turgor-related signals equally limit stomatal opening (Rodriguez-Dominguez, 2014), although this observation remains to be more widely tested.

4.3. Future directions

The approach presented here can be applied to any broad-leaved species, in principle, given its robust physiological basis. More importantly, it captures the plant response to moderate drought levels and, hence, the range in which stomata play its pivotal role. This extends the use of this plant-based sensor to conditions of moderate changes of soil water content, as already pointed out by other authors that raised the need to differentiate plant water status within low water stress conditions (Marino et al., 2016). Other plant-based measurements, like midday leaf or stem water potential, have limited value as water stress indicators under these conditions, because species like olive tend to maintain constant their minimum ψ under moderate soil water deficit (Cuevas et al., 2010; Diaz-Espejo et al., 2018; Fernández, 2014b). However, it is under such conditions that stomata exert most of their control on transpiration (Hernandez-Santana et al., 2016; López-Bernal et al., 2015), photosynthesis (Perez-Martin et al., 2014), fruit dry matter accumulation (Hernandez-Santana et al., 2018), and ultimately yield (Hernandez-Santana et al., 2017) in olive orchards, making the derivation of moderate water stress indicators highly valuable.

Our approach can be applied not only to optimize deficit irrigation strategies in crops, but also, as it targets on the monitoring of $g_{s,max}$, to more physiologically and ecologically based studies. For precision agriculture application, it is well known that previous studies on the heterogeneity of the experimental site (e.g. using remote sensing) greatly reduce the number of sensors to be used, decreasing the problematic of monitoring extended areas (Fernández, 2017, 2014a). For more eco-physiological studies, for instance, g_s optimization within plant canopies (Buckley et al., 2014) or plant physiological responses to different light conditions between shrub species (Díaz-Barradas et al., 2017), our physiological-based indicator of water stress levels may combine with them to automatically monitor differences in $g_{s,max}$ within their specific experimental goals, e.g. how $g_{s,max}$ is distributed within plant canopies, or how different are $g_{s,max}$ values from shaded or sunny leaves. Studies like this will largely contribute to expand data under a more widely range of environments and species, helping us to better infer g_s functioning. Thus, another step beyond for the physiological understanding of how g_s is controlled, is the combination of physiologically-based indicators with simplifications of mechanistic models of g_s, allowing to directly test specific processes in the field (Buckley et al., 2012; Diaz-Espejo et al., 2012). For instance, our indicator, *dZ/dD*, could be used to drive the BMF model (Buckley et al., 2003), the most mechanistic approach to model g_s currently, and, hence, to predict stomatal function under different scenarios of drought and high atmospheric demand.

A possible limitation of our approach that may seem to curtail its potential to monitor continuously and automatically $g_{s,max}$, could be identified on the necessity to wait until the end of the season to normalize and process the data. However, this was only needed for the present study (i) to be able to pool all ZIM probe output data together, since the experiment was not specifically designed to relate ZIM probe outputs to $g_{s,max}$, and (ii) to demonstrate the physiological foundation of *dZ/dD vs.* $g_{s,max}$. The normalization procedure presented here does not affect the diurnal dynamics of the ZIM probe output (P_p). Thus, the actual P_p can be perfectly used, together with *D* measurements, to conduct experiments in individual plants aiming at deriving a daily and automatic estimation of $g_{s,max}$, expanding the potential applications of our approach (see also Eqn A5 in which leaf turgor pressure, and not its normalized value, is related to g_s). The assessment of this potentiality

deserves more attention, and experiments specifically designed for that purpose will definitely expand the use of the automatic monitoring of $g_{s,max}$ from the leaf turgor proxy as a plant water stress indicator.

5. Conclusions

Plant response to drought is a highly demanding knowledge needed to overcome water scarcity and optimize agricultural water use. Understanding stomatal function and how it is controlled is crucial for that purpose. Here, we have demonstrated that the use of a plant-based sensor that measures a surrogate of leaf turgor pressure can be used to infer the large variability in maximum stomatal conductance under moderate drought conditions in an olive hedgerow orchard. The sensitivity of normalized leaf turgor to changes in D (dZ/dD), captured by the ZIM probes, is tightly related to $g_{s,max}$, which represents one of the best indicator of plant water stress. dZ/dD not only correlated significantly with $g_{s,max}$ under moderate water stress conditions during three consecutive seasons, but also it further supported the maximum canopy stomatal conductance estimation from sap flux density data. In addition, variations of dZ/dD *vs.* $g_{s,max}$ were linked to their underlying physiological traits (namely, the seasonal maximum transpiration rate, which depends on plant hydraulic conductance and minimum leaf water potential). The numerous applications of the plant water stress indicator presented here may range from precision crop irrigation management to more ecologically based studies, being of high interest for the scientist community exploring the effects of drought in plants.

Acknowledgements

This work was funded by the Spanish Ministry of Science and Innovation (research project AGL2009-11310/AGR) and co-funded by FEDER programme. C. M. R-D benefited from a FPDI research fellowship from the Junta de Andalucía during the data gathering and from an Individual Fellowship from the European Union's Horizon 2020 research and innovation programme under the Marie Skłodowska-Curie grant agreement No. 751918-AgroPHYS during the writing process of the manuscript. TNB was supported by the National Science Foundation (Award 1557906) and by the USDA National Institute of Food and Agriculture, Hatch project 1016439. We are grateful to the members of the Irrigation and Crop Ecophysiology group from IRNAS-CSIC for assistance in the field, especially to Antonio Montero and Alfonso Perez-Martin, and to Alfonso de Cires for helping on osmotic pressure measurements. We also thank the owners of Internacional Olivarera, S.A.U. (Interoliva) for allowing us to conduct the experiments in the Sanabria orchard, and Tim J. Brodribb for constructive inputs.

Appendix

We derive here a relationship between diurnal maximum stomatal conductance, $g_{s,max}$, and the normalized sensitivity of leaf turgor pressure, P, to leaf-to-air water vapor mole fraction difference, D. P is given by

$$P = \psi_{leaf} + \pi \tag{A1}$$

where ψ_{leaf} and π are leaf water potential and osmotic pressure ($\pi \geq 0$), respectively. ψ_{leaf} is given by

$$\psi_{leaf} = \psi_{soil} - \frac{g_s D}{K} \tag{A2}$$

where ψ_{soil} is soil water potential and K is soil-to-leaf hydraulic conductance. Combining A1 and A2 gives

$$P = \psi_{soil} + \pi - \frac{g_s D}{K} \tag{A3}$$

Differentiating P with respect to D gives

$$\frac{dP}{dD} = \frac{d\pi}{dD} - \frac{g_s}{K} - \frac{D}{K}\frac{dg_s}{dD} + \frac{g_s D}{K^2}\frac{dK}{dD} \tag{A4}$$

If π and K do not vary diurnally (as we found in the present study within irrigation treatments), their derivatives can be eliminated from A4. Rearranging then gives

$$\frac{dP}{dD} = -\frac{g_s}{K}\left(1 + \frac{d\ln g_s}{d\ln D}\right) \tag{A5}$$

(Note that $d\ln g_s/d\ln D$ is a total derivative, not a partial derivative; whereas the partial derivative would generally be negative, reflecting stomatal closure in response to increasing D, the total derivative can be positive if other factors are enhancing stomatal opening while D happens to be increasing – for example, if both PPFD and D are increasing during the morning, g_s may be increasing despite the increase in D, in which case $d\ln g_s/d\ln D$ would be positive.) As the derivation of normalized ZIM probe output (Z) was necessary in the present work, to relate dP/dD to Z, we must normalize dP/dD by the seasonal range in turgor, P_{max} - P_{min}. The seasonal maximum turgor will occur when transpiration rate is negligible at night, in which case leaf and soil water potentials are equal and $P = \psi_{soil} + \pi$. Thus, $P_{max} = \psi_{soil} + \pi$. The seasonal minimum P will occur when transpiration rate, E ($g_s D$), is at its maximum, E_{max}, so $P_{min} = \psi_{soil} + \pi - E_{max}/K$. The difference between P_{max} and P_{min} is simply E_{max}/K. Thus, normalized P (P_{rel}) is

$$P_{rel} = \frac{P - P_{min}}{P_{max} - P_{min}} = P\frac{K}{E_{max}} - P_{min}\frac{K}{E_{max}}$$

Differentiating P_{rel} with respect to D (again assuming K is diurnally invariant) and applying Eqn A5 gives

$$\frac{dP_{rel}}{dD} = \frac{K}{E_{max}}\frac{dP}{dD} = -\frac{g_s}{E_{max}}\left(1 + \frac{d\ln g_s}{d\ln D}\right) \tag{A7}$$

When g_s is at its diurnal maximum, its total derivative with respect to any given parameter is by definition zero, so $d\ln g_s/d\ln D = 0$. Thus

$$\frac{dP}{dD} = -\frac{g_{s,max}}{E_{max}} \tag{A8}$$

Normalized ZIM probe output, Z, can be used as a proxy for dP_{rel}/dD, and therefore for $g_{s,max}$. However, because ZIM probe output, P_p, is negatively related to leaf turgor, P (i.e., $dZ/dP < 0$ in State I), the signs of dZ/dD and dP/dD are reversed from one another, so that the normalized sensitivity of P to D given by Eq. (A7) will scale positively with dZ/dD. To a first approximation, P_p is negatively proportional to P, i.e., $P_p \approx b - mP$, with b and m constants unique to each probe installation. Thus $P_{p,max} \approx b - mP_{min}$ and $P_{p,min} \approx b - mP_{max}$, giving Z as

$$Z = \frac{P_p - P_{p,min}}{P_{p,max} - P_{p,min}} \approx \frac{(b - mP) - (b - mP_{max})}{(b - mP_{min}) - (b - mP_{max})} = \frac{P_{max} - P}{P_{max} - P_{min}} = 1 - \frac{P - P_{min}}{P_{max} - P_{min}} = 1 - P_{rel} \quad (A9)$$

Thus, $dZ/dP \propto -dP_{rel}/dD$, and

$$\frac{dZ}{dD} \propto \frac{g_{s,max}}{E_{max}} \quad (A10)$$

We found E_{max} to be conservative over each growing season (Supporting Information File Figure S1, S2), which implies that the slope of dZ/dD *vs.* $g_{s,max}$ should likewise be conservative. In cases where E_{max} is not conservative, its variations may be predicted and/or interpreted in terms of underlying physiological traits: E_{max} depends on K and on minimum ψ_{leaf}, as

$$E_{max} = K(\psi_{soil} - \psi_{leaf,min}) \quad (A11)$$

Thus, the slope relating dP_{rel}/dD, and thus dZ/dD, to $g_{s,max}$ should be smaller if leaf hydraulic conductance or soil water potential are greater, and the slope should be greater if seasonal minimum leaf water potential is more negative.

Appendix A. Supplementary data

Supplementary material related to this article can be found, in the online version, at doi:https://doi.org/10.1016/j.agrformet.2019.04.006.

References

Ache, P., Bauer, H., Kollist, H., Al-Rasheid, Ka S., Lautner, S., Hartung, W., Hedrich, R., 2010. Stomatal action directly feeds back on leaf turgor: new insights into the regulation of the plant water status from non-invasive pressure probe measurements. Plant J. 62, 1072–1082. https://doi.org/10.1111/j.1365-313X.2010.04213.x.

Allen, R., Pereira, L., Raes, D., Smith, M., 1998. Crop Evapotranspiration - Guidelines for Computing Crop Water Requirements. FAO Irrigation and Drainage Paper 56. Rome, Italy.

Bader, M.K.-F., Ehrenberger, W., Bitter, R., Stevens, J., Miller, B.P., Chopard, J., Rüger, S., Hardy, G.E.S.J., Poot, P., Dixon, K.W., Zimmermann, U., Veneklaas, E.J., 2014. Spatio-temporal water dynamics in mature Banksia menziesii trees during drought. Physiol. Plant. 152, 301–315. https://doi.org/10.1111/ppl.12170.

Bartlett, M.K., Scoffoni, C., Ardy, R., Zhang, Y., Sun, S., Cao, K., Sack, L., 2012. Rapid determination of comparative drought tolerance traits: using an osmometer to predict turgor loss point. Methods Ecol. Evol. 3, 880–888. https://doi.org/10.1111/j.2041-210X.2012.00230.x.

Bauer, H., Ache, P., Lautner, S., Fromm, J., Hartung, W., Al-Rasheid, K.A.S., Sonnewald, S., Sonnewald, U., Kneitz, S., Lachmann, N., Mendel, R.R., Bittner, F., Hetherington, A.M., Hedrich, R., 2013. The stomatal response to reduced relative humidity requires guard cell-autonomous ABA synthesis. Curr. Biol. 23, 53–57. https://doi.org/10.1016/j.cub.2012.11.022.

Bramley, H., Ehrenberger, W., Zimmermann, U., Palta, Ja., Rüger, S., Siddique, K.H.M., 2013. Non-invasive pressure probes magnetically clamped to leaves to monitor the water status of wheat. Plant Soil 369, 257–268. https://doi.org/10.1007/s11104-012-1568-x.

Buck, A.L., 1981. New equations for computing vapor pressure and enhancement factor. J. Appl. Meteorol. 20, 1527–1532. https://doi.org/10.1175/1520-0450(1981)020<1527:NEFCVP>2.0.CO;2.

Buckley, T.N., 2005. The control of stomata by water balance. New Phytol. 168, 275–292. https://doi.org/10.1111/j.1469-8137.2005.01543.x.

Buckley, T.N., 2017. Modeling stomatal conductance. Plant Physiol. 174, 572–582. https://doi.org/10.1104/pp.16.01772.

Buckley, T.N., Mott, K.A., 2013. Modelling stomatal conductance in response to environmental factors. Plant Cell Environ. 36, 1691–1699. https://doi.org/10.1111/pce.12140.

Buckley, T.N., Mott, K.A., Farquhar, G.D., 2003. A hydromechanical and biochemical model of stomatal conductance. Plant Cell Environ. 26, 1767–1785. https://doi.org/10.1046/j.1365-3040.2003.01094.x.

Buckley, T.N., Turnbull, T.L., Adams, M.A., 2012. Simple models for stomatal conductance derived from a process model: cross-validation against sap flux data. Plant Cell Environ. 35, 1647–1662. https://doi.org/10.1111/j.1365-3040.2012.02515.x.

Buckley, T.N., Martorell, S., Diaz-Espejo, A., Tomàs, M., Medrano, H., 2014. Is stomatal conductance optimized over both time and space in plant crowns? A field test in grapevine (Vitis vinifera). Plant Cell Environ. 37, 2707–2721. https://doi.org/10.1111/pce.12343.

Conejero, W., Alarcón, J.J., García-Orellana, Y., Nicolás, E., Torrecillas, A., 2007. Evaluation of sap flow and trunk diameter sensors for irrigation scheduling in early maturing peach trees. Tree Physiol. 27, 1753–1759.

Core Team, R., 2017. R: A Language and Environment for Statistical Computing. R Foundation for Statistical Computing.

Correia, M.J., Pereira, J.S., Chaves, M.M., Rodrigues, M.L., Pacheco, C.A., 1995. ABA xylem concentrations determine maximum daily leaf conductance of field-grown Vitis vinifera L. plants. Plant Cell Environ. 18, 511–521. https://doi.org/10.1111/j.1365-3040.1995.tb00551.x.

Cuevas, M.V., Torres-Ruiz, J.M., Álvarez, R., Jiménez, M.D., Cuerva, J., Fernández, J.E., 2010. Assessment of trunk diameter variation derived indices as water stress indicators in mature olive trees. Agric. Water Manag. 97, 1293–1302. https://doi.org/10.1016/j.agwat.2010.03.011.

Cuevas, M.V., Martín-Palomo, M.J., Diaz-Espejo, A., Torres-Ruiz, J.M., Rodriguez-Dominguez, C.M., Perez-Martin, A., Pino-Mejías, R., Fernández, J.E., 2013. Assessing water stress in a hedgerow olive orchard from sap flow and trunk diameter measurements. Irrig. Sci. 31, 729–746. https://doi.org/10.1007/s00271-012-0357-x.

Damour, G., Simonneau, T., Cochard, H., Urban, L., 2010. An overview of models of stomatal conductance at the leaf level. Plant Cell Environ. 33, 1419–1438. https://doi.org/10.1111/j.1365-3040.2010.02181.x.

Díaz-Barradas, M.C., Zunzunegui, M., Alvarez-Cansino, L., Esquivias, M.P., Valera, J., Rodríguez, H., 2017. How do Mediterranean shrub species cope with shade? Ecophysiological response to different light intensities. Plant Biol. 20, 296–306. https://doi.org/10.1111/plb.12661.

Diaz-Espejo, A., Buckley, T.N., Sperry, J.S., Cuevas, M.V., de Cires, A., Elsayed-Farag, S., Martin-Palomo, M.J., Muriel, J.L., Perez-Martin, A., Rodriguez-Dominguez, C.M., Rubio-Casal, A.E., Torres-Ruiz, J.M., Fernández, J.E., 2012. Steps toward an improvement in process-based models of water use by fruit trees: a case study in olive. Agric. Water Manag. 114, 37–49. https://doi.org/10.1016/j.agwat.2012.06.027.

Diaz-Espejo, A., Fernández, J.E., Torres-Ruiz, J.M., Rodriguez-Dominguez, C.M., Perez-Martin, A., Hernandez-Santana, V., 2018. The olive tree under Water stress. Water Scarcity and Sustainable Agriculture in Semiarid Environment. Elsevier, pp. 439–479. https://doi.org/10.1016/B978-0-12-813164-0.00018-1.

Dreux, R., Fernandes, M., Victoria, M., Hernandez-santana, V., Rodriguez-dominguez, C.M., Padilla-díaz, C.M., Enrique, J., 2017. Classification models for automatic identification of daily states from leaf turgor related measurements in olive. Comput. Electron. Agric. 142, 181–189. https://doi.org/10.1016/j.compag.2017.09.005.

Ehrenberger, Rüger, S., Fitzke, R., Vollenweider, P., Günthardt-Goerg, M., Kuster, T., Zimmermann, U., Arend, M., 2012a. Concomitant dendrometer and leaf patch pressure probe measurements reveal the effect of microclimate and soil moisture on diurnal stem water and leaf turgor variations in young oak trees. Funct. Plant Biol. 39, 297. https://doi.org/10.1071/FP11206.

Ehrenberger, Rüger, S., Rodríguez-Domínguez, C.M., Díaz-Espejo, A., Fernández, J.E., Moreno, J., Zimmermann, D., Sukhorukov, V.L., Zimmermann, U., 2012b. Leaf patch clamp pressure probe measurements on olive leaves in a nearly turgorless state. Plant Biol. (Stuttg). 14, 666–674. https://doi.org/10.1111/j.1438-8677.2011.00545.x.

Fernández, J.E., 2014a. Plant-based sensing to monitor water stress: applicability to commercial orchards. Agric. Water Manag. 142, 99–109. https://doi.org/10.1016/j.agwat.2014.04.017.

Fernández, J.E., 2014b. Understanding olive adaptation to abiotic stresses as a tool to increase crop performance. Environ. Exp. Bot. 103, 158–179. https://doi.org/10.1016/j.envexpbot.2013.12.003.

Fernández, J.E., 2017. Plant-based methods for irrigation scheduling of woody crops. Horticulturae 3, 35. https://doi.org/10.3390/horticulturae3020035.

Fernández, J.E., Moreno, F., Girón, I.F., Blázquez, O.M., 1997. Stomatal control of water use in olive tree leaves. Plant Soil 190, 179–192.

Fernández, J.E., Palomo, M., Diaz-Espejo, A., Clothier, B., Green, S., Girón, I., Moreno, F., 2001. Heat-pulse measurements of sap flow in olives for automating irrigation: tests, root flow and diagnostics of water stress. Agric. Water Manag. 51, 99–123. https://doi.org/10.1016/S0378-3774(01)00119-6.

Fernández, J.E., Durán, P.J., Palomo, M.J., Diaz-Espejo, A., Girón, I.F., 2006. Calibration

of sap flow estimated by the compensation heat pulse method in olive, plum and orange trees: relationships with xylem anatomy. Tree Physiol. 26, 719–728.
Fernández, J.E., Green, S.R., Caspari, H.W., Diaz-Espejo, A., Cuevas, M.V., 2008. The use of sap flow measurements for scheduling irrigation in olive, apple and Asian pear trees and in grapevines. Plant Soil 305, 91–104. https://doi.org/10.1007/s11104-007-9348-8.
Fernández, J.E., Rodriguez-Dominguez, C.M., Perez-Martin, A., Zimmermann, U., Rüger, S., Martín-Palomo, M.J., Torres-Ruiz, J.M., Cuevas, M.V., Sann, C., Ehrenberger, W., Diaz-Espejo, A., 2011. Online-monitoring of tree water stress in a hedgerow olive orchard using the leaf patch clamp pressure probe. Agric. Water Manag. 100, 25–35. https://doi.org/10.1016/j.agwat.2011.08.015.
Fernández, J.E., Perez-Martin, A., Torres-Ruiz, J.M., Cuevas, M.V., Rodriguez-Dominguez, C.M., Elsayed-Farag, S., Morales-Sillero, A., García, J.M., Hernandez-Santana, V., Diaz-Espejo, A., 2013. A regulated deficit irrigation strategy for hedgerow olive orchards with high plant density. Plant Soil 372, 279–295. https://doi.org/10.1007/s11104-013-1704-2.
Fernández, J.E., Diaz-Espejo, A., Romero, R., Hernandez-Santana, V., García, J.M., Padilla-Díaz, C.M., Cuevas, M.V., 2018. Precision irrigation in olive (Olea europaea L.) Tree orchards. Water Scarcity and Sustainable Agriculture in Semiarid Environment. Elsevier, pp. 179–217. https://doi.org/10.1016/B978-0-12-813164-0.00009-0.
Flexas, J., Medrano, H., 2002. Drought-inhibition of photosynthesis in C3 plants: stomatal and non-stomatal limitations revisited. Ann. Bot. 89, 183–189. https://doi.org/10.1093/aob/mcf027.
Flexas, J., Bota, J., Cifre, J., Escalona, J.M., Galmés, J., Gulías, J., Lefi, E.K., Martínez-Cañellas, S.F., Moreno, M.T., Ribas-Carbó, M., Riera, D., Sampol, B., Medrano, H., 2004. Understanding down-regulation of photosynthesis under water stress: future prospects and searching for physiological tools for irrigation management. Ann. Appl. Biol. 144, 273–283. https://doi.org/10.1111/j.1744-7348.2004.tb00343.x.
Green, S., Clothier, B., Jardine, B., 2003. Theory and practical application of heat pulse to measure sap flow. Agron. J. 95, 1371–1379.
Hernandez-Santana, V., Fernández, J.E., Rodriguez-Dominguez, C.M., Romero, R., Diaz-Espejo, A., 2016. The dynamics of radial sap flux density reflects changes in stomatal conductance in response to soil and air water deficit. Agric. For. Meteorol 218–219, 92–101. https://doi.org/10.1016/j.agrformet.2015.11.013.
Hernandez-Santana, V., Fernández, J.E., Cuevas, M.V., Perez-Martin, A., Diaz-Espejo, A., 2017. Photosynthetic limitations by water deficit: effect on fruit and olive oil yield, leaf area and trunk diameter and its potential use to control vegetative growth of super-high density olive orchards. Agric. Water Manag. 184, 9–18. https://doi.org/10.1016/j.agwat.2016.12.016.
Hernandez-Santana, V., Fernandes, R.D.M., Perez-Arcoiza, A., Fernández, J.E., Garcia, J.M., Diaz-Espejo, A., 2018. Relationships between fruit growth and oil accumulation with simulated seasonal dynamics of leaf gas exchange in the olive tree. Agric. For. Meteorol 256–257, 458–469. https://doi.org/10.1016/j.agrformet.2018.03.019.
Hetherington, A.M., Woodward, F.I., 2003. The role of stomata in sensing and driving environmental change. Nature 424, 901–908. https://doi.org/10.1038/nature01843.
Intrigliolo, D.S., Castel, J.R., 2006. Performance of various water stress indicators for prediction of fruit size response to deficit irrigation in plum. Agric. Water Manag. 83, 173–180. https://doi.org/10.1016/j.agwat.2005.12.005.
Jarvis, P.G., Mcnaughton, K.G., 1986. Stomatal control of transpiration: scaling up from leaf to region. Adv. Ecol. Res. 15, 1–49. https://doi.org/10.1016/S0065-2504(08)60119-1.
Jones, H.G., 2007. Monitoring plant and soil water status: established and novel methods revisited and their relevance to studies of drought tolerance. J. Exp. Bot. 58, 119–130. https://doi.org/10.1093/jxb/erl118.
Lee, K.M., Driever, S.M., Heuvelink, E., Rüger, S., Zimmermann, U., de Gelder, A., Marcelis, L.F.M., 2012. Evaluation of diel patterns of relative changes in cell turgor of tomato plants using leaf patch clamp pressure probes. Physiol. Plant. 146, 439–447. https://doi.org/10.1111/j.1399-3054.2012.01637.x.
López-Bernal, Á., García-Tejera, O., Vega, V.A., Hidalgo, J.C., Testi, L., Orgaz, F., Villalobos, F.J., 2015. Using sap flow measurements to estimate net assimilation in olive trees under different irrigation regimes. Irrig. Sci. 33, 357–366. https://doi.org/10.1007/s00271-015-0471-7.
López-Bernal, A., García-Tejera, O., Testi, L., Orgaz, F., Villalobos, F.J., 2018. Stomatal oscillations in olive trees: analysis and methodological implications. Tree Physiol. 38, 531–542. https://doi.org/10.1093/treephys/tpx127.
Marino, G., Pernice, F., Marra, F.P., Caruso, T., 2016. Validation of an online system for the continuous monitoring of tree water status for sustainable irrigation managements in olive (Olea europaea L.). Agric. Water Manag. 177, 298–307. https://doi.org/10.1016/j.agwat.2016.08.010.
Martínez-Gimeno, M.A., Castiella, M., Rüger, S., Intrigliolo, D.S., Ballester, C., 2017. Evaluating the usefulness of continuous leaf turgor pressure measurements for the assessment of Persimmon tree water status. Irrig. Sci. 35, 159–167. https://doi.org/10.1007/s00271-016-0527-3.
Martin-StPaul, N., Delzon, S., Cochard, H., 2017. Plant resistance to drought depends on timely stomatal closure. Ecol. Lett. 116, 519–532. https://doi.org/10.1111/ele.12851.
McAdam, S.A.M., Brodribb, T.J., 2014. Separating Active and Passive Influences on Stomatal Control of Transpiration[OPEN]. Plant Physiol. 164, 1578–1586. https://doi.org/10.1104/pp.113.231944.
McAdam, S.A.M., Brodribb, T.J., 2015. The evolution of mechanisms driving the stomatal response to vapor pressure deficit. Plant Physiol. 167, 833–843. https://doi.org/10.1104/pp.114.252940.
McAdam, S.A.M., Brodribb, T.J., 2016. Linking turgor with ABA biosynthesis: implications for stomatal responses to vapour pressure deficit across land plants. Plant Physiol. 171, 00380. https://doi.org/10.1104/pp.16.00380. 2016.
Medrano, H., Escalona, J.M., Bota, J., Gulías, J., Flexas, J., 2002. Regulation of photosynthesis of C3 plants in response to progressive drought: stomatal conductance as a reference parameter. Ann. Bot. 89, 895–905. https://doi.org/10.1093/aob/mcf079.
Muggeo, V.M.R., 2003. Estimating regression models with unknown break-points. Stat. Med. 22, 3055–3071. https://doi.org/10.1002/sim.1545.
Muggeo, V.M.R., 2008. Segmented: an R package to fit regression models with broken-line relationships. R News 8, 20–25.
Ortuño, M.F., Conejero, W., Moreno, F., Moriana, A., Intrigliolo, D.S., Biel, C., Mellisho, C.D., Pérez-Pastor, A., Domingo, R., Ruiz-Sánchez, M.C., 2010. Could trunk diameter sensors be used in woody crops for irrigation scheduling? A review of current knowledge and future perspectives. Agric. Water Manag. 97, 1–11. https://doi.org/10.1016/j.agwat.2009.09.008.
Padilla-Díaz, C.M., Rodriguez-Dominguez, C.M., Hernandez-Santana, V., Perez-Martin, A., Fernández, J.E., 2016. Scheduling regulated deficit irrigation in a hedgerow olive orchard from leaf turgor pressure related measurements. Agric. Water Manag. 164, 28–37. https://doi.org/10.1016/j.agwat.2015.08.002.
Padilla-Díaz, C.M., Rodriguez-Dominguez, C.M., Hernandez-Santana, V., Perez-Martin, A., Fernandes, R.D.M., Montero, A., García, J.M., Fernández, J.E., 2018. Water status, gas exchange and crop performance in a super high density olive orchard under deficit irrigation scheduled from leaf turgor measurements. Agric. Water Manag. 202, 241–252. https://doi.org/10.1016/j.agwat.2018.01.011.
Perez-Martin, A., Michelazzo, C., Torres-Ruiz, J.M., Flexas, J., Fernández, J.E., Sebastiani, L., Diaz-Espejo, A., 2014. Regulation of photosynthesis and stomatal and mesophyll conductance under water stress and recovery in olive trees: correlation with gene expression of carbonic anhydrase and aquaporins. J. Exp. Bot. 65, 3143–3156. https://doi.org/10.1093/jxb/eru160.
Rodriguez-Dominguez, C.M., 2014. The Control of Transpiration in Olive and Almond: Mechanisms Under Drought Conditions. PhD Thesis. http://hdl.handle.net/11441/23509.
Rodriguez-Dominguez, C.M., Ehrenberger, W., Sann, C., Rüger, S., Sukhorukov, V., Martín-Palomo, M.J., Diaz-Espejo, A., Cuevas, M.V., Torres-Ruiz, J.M., Perez-Martin, A., Zimmermann, U., Fernández, J.E., 2012. Concomitant measurements of stem sap flow and leaf turgor pressure in olive trees using the leaf patch clamp pressure probe. Agric. Water Manag. 114, 50–58. https://doi.org/10.1016/j.agwat.2012.07.007.
Rodriguez-Dominguez, C.M., Buckley, T.N., Egea, G., de Cires, A., Hernandez-Santana, V., Martorell, S., Diaz-Espejo, A., 2016. Most stomatal closure in woody species under moderate drought can be explained by stomatal responses to leaf turgor. Plant Cell Environ. 39, 2014–2026. https://doi.org/10.1111/pce.12774.
Rodriguez-Dominguez, C.M., Carins Murphy, M.R., Lucani, C., Brodribb, T.J., 2018. Mapping xylem failure in disparate organs of whole plants reveals extreme resistance in olive roots. New Phytol. 218, 1025–1035. https://doi.org/10.1111/nph.15079.
Rogers, A., Medlyn, B.E., Dukes, J.S., Bonan, G., von Caemmerer, S., Dietze, M.C., Kattge, J., Leakey, A.D.B., Mercado, L.M., Niinemets, Ü., Prentice, I.C., Serbin, S.P., Sitch, S., Way, D.A., Zaehle, S., 2017. A roadmap for improving the representation of photosynthesis in Earth system models. New Phytol. 213, 22–42. https://doi.org/10.1111/nph.14283.
Rüger, S., Ehrenberger, W., Arend, M., Geßner, P., Zimmermann, G., Zimmermann, D., Bentrup, F.-W., Nadler, a., Raveh, E., Sukhorukov, V.L., 2010a. Comparative monitoring of temporal and spatial changes in tree water status using the non-invasive leaf patch clamp pressure probe and the pressure bomb. Agric. Water Manag. 98, 283–290. https://doi.org/10.1016/j.agwat.2010.08.022.
Rüger, S., Netzer, Y., Westhoff, M., Zimmermann, D., Reuss, R., Ovadiya, S., Gessner, P., Zimmermann, G., Schwartz, a., Zimmermann, U., 2010b. Remote monitoring of leaf turgor pressure of grapevines subjected to different irrigation treatments using the leaf patch clamp pressure probe. Aust. J. Grape Wine Res. 16, 405–412. https://doi.org/10.1111/j.1755-0238.2010.00101.x.
Torres-Ruiz, J.M., Diaz-Espejo, A., Morales-Sillero, A., Martín-Palomo, M.J., Mayr, S., Beikircher, B., Fernández, J.E., 2013. Shoot hydraulic characteristics, plant water status and stomatal response in olive trees under different soil water conditions. Plant Soil 373, 77–87. https://doi.org/10.1007/s11104-013-1774-1.
Westhoff, M., Reuss, R., Zimmermann, D., Netzer, Y., Gessner, A., Gessner, P., Zimmermann, G., Wegner, L.H., Bamberg, E., Schwartz, a, Zimmermann, U., 2009. A non-invasive probe for online-monitoring of turgor pressure changes under field conditions. Plant Biol. (Stuttg). 11, 701–712. https://doi.org/10.1111/j.1438-8677.2008.00170.x.
Zimmermann, D., Reuss, R., Westhoff, M., Gessner, P., Bauer, W., Bamberg, E., Bentrup, F.-W., Zimmermann, U., 2008. A novel, non-invasive, online-monitoring, versatile and easy plant-based probe for measuring leaf water status. J. Exp. Bot. 59, 3157–3167. https://doi.org/10.1093/jxb/ern171.